

Applying Vermiculite-Modified Polypropylene Film to Flexible Packaging Material

YaBo Fu, DongLi Li, WenCai Xu, YingQun Qi, Wei Shang, WeiXia Wu, YaJun Wang

Beijing Key Laboratory of Printing & Packaging Materials and Technology, College of Printing and Packaging, Beijing Institute of Graphic Communication, Beijing 102600, People's Republic of China

Correspondence to: D. L. Li (E-mail: lidongli@bigc.edu.cn)

ABSTRACT: This article presents a process for preparing organovermiculite by ball-milling expanded vermiculite (EVMT) in water-based ethylene vinyl acetate (EVA) latex. In this process, the vermiculite (VMT) is exfoliated to prepare a kind of EVMT/EVA modifying agent, in which EVA serves as both intercalating polymer into VMT and compatibilizer between VMT and polypropylene (PP). During melt blending between EVMT/EVA and PP, shear force exfoliates VMT sheets, dispersing them relatively well in the PP matrix. Compared with raw PP, EVMT-modified cast polypropylene (CPP) are better when EVMT loading ranged from 0.5 to 1.0%, with improvement in both the strength and toughness of the EVMT/EVA-modified CPP film. Specifically, tensile strength was increased by 44–54%, yield stress increased by 26%, stress at break increased by 37–43%, energy at break (toughness) increased by 29–34%, oxygen transmission rate decreased by 6.2–12.9%, the water vapor transmission rate was not significantly affected, the peel bond strength of laminated CPP film increased by 18–27%, and the processability and melt flow index (MFI) of EVMT/EVA/PP composites were improved as well. Increasing MFI attributes facilitated the processing and formation of EVMT/EVA/PP. © 2014 Wiley Periodicals, Inc. *J. Appl. Polym. Sci.* **2014**, *131*, 40954.

KEYWORDS: composites; films; mechanical properties; packaging; X-ray

Received 14 January 2014; accepted 4 May 2014

DOI: 10.1002/app.40954

INTRODUCTION

The global consumer flexible-packaging market was worth an estimated \$18.1 million in 2011 and is predicted to reach \$22.5 million by 2016, according to a report by PIRA International.¹ According to the report, the market for flexible plastics, particularly polyethylene (PE) and polypropylene (PP), will grow quickly, so will higher-barrier plastics such as biaxially oriented polyethylene terephthalate (BOPET), ethylene vinyl alcohol (EVOH), and polyamide (PA). With advantages such as low cost, good water resistance, hot sealability, and printability, PP accounts for 32% of raw plastic films at present, among which biaxially oriented polypropylene (BOPP) and cast polypropylene (CPP) account for 26.5 and 5.5%, respectively. Despite its advantages, PP has also several urgent problems to address:

- PP film has extremely low polarity and thus low intermolecular force, making for highly polar ink or adhesive; this leads to poor ink adhesion and low peel strength of composite films;
- PP's poor barrier capability against oxygen makes it necessary to compound it with higher barrier plastics such as BOPET, EVOH, and PA to enhance its oxygen barrier properties; and

- Low tensile strength, small modulus of elasticity (Young's modulus), and large tensional deformation of films make PP prone to misregistration (being out of register) or warpage after lamination.

Such imperfect properties of PP are generally improved by modifying it, and a good way of enhancing its mechanical and barrier properties is the use of nanosized clay-modified PP. Using relatively low loading of clay, many of the composites' physical and chemical properties have been improved significantly, as compared with the neat polymer. Both vermiculite (VMT) and montmorillonite (MMT) are of layered phyllosilicate clay, but they differ in type of interlayer ion and quantity of interlayer bound water. VMT is a mica-type silicate with 2 : 1 layered phyllosilicate; it has a large internal surface, high cation exchange capacity (CEC), and high negative charge on its silicate layers. VMT has a tetrahedral–octahedral–tetrahedral layer (or sheet) and an interlayer (or gallery), and the thickness of the structural unit (2 : 1 layer and interlayer space; basal spacing) is up to 1.4 nm, depending on the interlamellar water layer and the interlayer cation.² When instantaneously heated, VMT sheets will be quickly dehydrated, and expand to form the expanded vermiculite (EVMT) with large interlayer spacing,

macromolecules is more likely to be inserted into EVMT than MMT, and consequently EVMT serves as polymer modifier in this article. EVMT has certain degree of order, and it is not necessary to exfoliate VMT into single sheets. Under shear force, EVMT among polymer resin is exfoliated into single sheets with large aspect ratio, which will give rise to significant improvement in polymer performance. For instance, Shao et al.³ demonstrated that modified with 8% VMT, PP's recrystallization temperature increased by 12°C; in addition, with VMT loading of 0.5%, PP's tensile strength increased by 10%, whereas its Young's modulus and Izod impact slightly fell. Pereira de Abreu et al.⁴ found that after 2.9% of nanoclay was added, PP's tensile strength remained unchanged and its Young's modulus rose by 70%, whereas its oxygen transmission rate (OTR) fell by 22%. Using 5% maleic anhydride (MAH)-modified PP as a compatibilizer, Han et al. added 1% VMT, as a result, the obtained PP exhibited a 25% higher tensile strength, a 14% rise in impact strength, and a 20% rise in flexural strength, while elongation at break hardly changed at all. These results indicate that PP toughness increases after being modified with VMT.⁵ Zhang et al.⁶ intercalated VMT with MAH and then grafted PP *in situ* to obtain the modified PP, and found that tensile strength increased by 12.8%, impact strength increased by 14%, and flexural strength increased by 20%.

VMT plays a major role in improving the mechanical and barrier properties of PP, as described above. However, a major problem pertaining to the aforementioned PP modification processes is that the VMT modifying agents used (e.g., MAH) are somewhat toxic. To allow VMT to be exfoliated or intercalated, some organoamines^{7,8} are usually used as intercalating agents; however, such organoamines are fairly toxic. Thus, modified PP films prepared by conventional modification processes are not suitable for food packaging material.

Ethylene vinyl acetate (EVA) is a kind of copolymer, whose main chain consists of two types of repeating units [ethylene and vinyl acetate (VA)], and its macromolecular structure is irregular; thus, it is an amorphous polymer. The weight percent of VA is 10–40%, with the remainder being ethylene. The polar VA segments are relatively well compatible with single sheets of EVMT.

In this study, we prepared a kind of nontoxic organovermiculite (OVMT) modifying agent based on natural EVMT in water-based EVA latex by means of ball-milling intercalation. Our method differs from those used in the literature available in the following aspects: (1) EVA copolymers, instead of an organoamine intercalating agent, are used; (2) EVA is directly intercalated into VMT to simplify the process, rather than modifying organic encapsulation of the VMT surface with a silane-based coupling agent after initial ion exchange; and (3) EVA latex serves as the starting material, which has a better intercalation effect than EVA resin adopted by many researchers in the melt blending process.^{9,10}

This process of directly intercalating EVA latex into VMT by ball milling is to be reported for the first time in the world. The purposes of this work are threefold: to synthesize OVMTs

by intercalation and encapsulation with EVA latex; to prepare OVMT nanocomposites based on PP (EVMT/EVA/PP) by melt blending; and to use casting equipment to prepare CPP film and to investigate the influences of EVMT/EVA content on the dispersion of VMT in the PP matrix, as well as the compounded CPP's crystallinity, mechanical properties, OTR, and peel strength.

EXPERIMENTAL

In our experiment, EVMT/EVA was characterized using X-ray diffraction (XRD). The cross-section morphologies of EVMT/EVA and the CPP films were examined using a scanning electron microscope (SEM). The crystallization behavior of CPP films was determined using a differential scanning calorimeter (DSC). The peel strength of composite film was tested with a universal testing machine. OTR and water vapor transmission rate (WVTR) were tested with an oxygen transmission analyzer and a water vapor transmission analyzer, respectively. The glass transition temperature and dynamic viscoelasticity of the modified CPP film were tested using dynamic mechanical analysis (DMA).

Materials

The natural VMT used in this study was taken from the Qeganbulak VMT deposit (Yuli County, Xinjiang, China). EVMT was obtained by instantaneously heating the raw natural VMT in a furnace at 1100°C. Its CEC is 98.6 mmol/100 g and its d-spacing is 14.93 Å (hydrated clay).

EVA latex was of grade BJ-707, with solid content of 55%, purchased from Beijing Organic Chemical Plant, Beijing, China.

The PP material was F280 PP dedicated for BOPP copolymer, purchased from Sinopec Maoming Petrochemical Company, Maoming, China.

Preparation and Characterization of EVMT/EVA

The procedure was as follows: EVMT was crushed in a high-speed pulverizer for 5 min, and sieved to get 50–100 mesh EVMT, then a certain mass of crushed EVMT was weighed and mixed with EVA latex at various ratios shown in Table I. Subsequently, the mixture was milled at a speed of 2000 rpm in a high-speed ball miller (GJ-28, Qingdao Haitong Special Instrument Co., Qingdao City, China) for various durations. Later, the VMT in latex was measured using a laser particle size analyzer (S3500, Microtrac, USA).

Table I shows that, with increasing ball-milling time, particle size of EVMT decreases gradually, and after ball milling for 5 h, the particle size reduction tends to be gentle; that EVMT/EVA sample subjected to 2 h ball milling and that subjected to 3 h ball milling are similar in mean particle size and particle size distribution; and that samples EVMT/EVA-5h and EVMT/EVA-7h are also close in mean particle size and particle size distribution. Therefore, we only chose samples EVMT/EVA-2h and EVMT/EVA-5h for analysis.

Take a small amount of the EVMT/EVA-2h and EVMT/EVA-5h latexes prepared as above, dry at 80°C for 2 h to yield the EVMT/EVA dry basis, and then determine crystallization structures of the EVMT, EVA, and EVMT/EVA samples using XRD.

Table I. Ball-Milling Treatment of EVMT in EVA Latex and Particle Size Distribution

Code of modifying agent	EVMT/EVA-2h	EVMT/EVA-3h	EVMT/EVA-5h	EVMT/EVA-7h
Ball milling time	2 h	3 h	5 h	7 h
Vermiculite : EVA latex ratio (by mass)	1 : 3	1 : 3	1 : 3	1 : 3
Mean particle size (μm)	3.91	3.66	2.80	2.32
Peak particle size (μm)	15.70	15.59	2.80	2.32
Range of particle size (80%; μm)	1.05 – 18.30	1.02 – 17.79	0.95 – 10.68	0.90 – 7.12

XRD patterns were recorded in a D/max2550HB+/PC X-ray diffractometer (Rigaku, Japan) with a graphite monochromator, using a Cu K α radiation source ($k = 0.154439$ nm) and operating at 40 kV/200 mA. The samples were scanned at the diffraction angle 2θ in the range of $1.5\text{--}50^\circ$ with a step size of 0.02° and a counting time of 10 s per step. The basal spacing of samples was determined from the diffraction peak, using the Bragg equation ($k = 2 d \sin \theta$).

Preparation of Nanocomposite Materials

In this study, melt blending was used to prepare EVMT/EVA/PP nanocomposites. The raw PP pellets and the EVMT/EVA were dried at 80°C for 2 h. Then, the mixtures of the raw PP pellets with various ratios of EVMT/EVA-2h (Table II) were fed into a twin-screw extruder [CTE-35, Coperion Keya (Nanjing) Machinery Co., China] preheated to $185\text{--}230^\circ\text{C}$. The screw rotation speed was maintained at 300 rpm. The extruded EVMT/EVA/PP nanocomposites were cut into small pieces and then made into CPP films.

Preparation and Analysis of CPP Films

The modified PP pellets were placed in the feeding hopper of a cast-film extruder (MLR-500, Labtech Engineering Co., Thailand). The four-stage heating temperature was set at 230°C , the extruding die temperature at 208°C , the extruding pressure at 45 bar, screw rotation speed at 48 rpm, cooling fan rotation speed at 1414 rpm, linear speed of the rewinding roller at 4.7 m/min, and the thickness of prepared cast film at 41 ± 1 μm .

Mechanical Properties. For this test, CPP samples were cut into dumbbell shapes. Every CPP dumbbell specimen was tested using a 5565A Instron universal testing machine (Instron, USA) at a crosshead speed of 50 mm/min, according to the ASTM

D638 standard.¹¹ The tensile testing machine pulls the sample from both ends and measures the force required to pull the specimen apart and how much the sample has been stretched before breaking. According to the stress and strain curve, the tensile strength, Young's modulus, yield stress, stress at break, elongation at break, and energy at break were obtained.

SEM Analysis. The morphology of each fractured cross-section was examined using a Shimadzu SS-550 SEM at an accelerating voltage of 15 kV. The brittle and ductile fractured cross-sections were prepared according to the following methods. (1) For brittle fractured surface: Put the material in liquid nitrogen and immerse for 2 min; remove it from the liquid nitrogen and break it with a heavy hammer and take the fractured surfaces to prepare cross-sections; then perform gold sputtering and testing. (2) For ductile fractured surface: Use an electronic tensile tester to stretch the sample bar at a rate of 30 mm/min until the plastic sample fractures; take the fractured surfaces to prepare cross-sections; and perform gold sputtering and testing.

DSC Analysis. The onset crystallization temperature (T_{on}), end-set crystallization temperature (T_{end}), crystallization temperature at peak (T_{peak}), and enthalpy of recrystallization (ΔH_c) were determined using a Netzsch DSC-200PC (Netzsch, Germany). The instrument was calibrated using indium as the standard. Each sample was prepared by sealing 5–10 mg material in an aluminum pan, and all experiments were performed under a nitrogen gas flow. The samples were heated from 30 to 210°C at a rate of $20^\circ\text{C}/\text{min}$, held for 5 min to erase any thermal history, then cooled to -50°C at a rate of $10^\circ\text{C}/\text{min}$ and held for 5 min; they were subsequently heated to 210°C at a rate of $20^\circ\text{C}/\text{min}$ and held for 5 min. The degree of crystallinity (X_c) of each specimen was calculated, assuming that the melting enthalpy of 100% crystalline PP is 165 J/g.¹²

Table II. Mechanical Properties of Modified CPP

Code	Component proportion (Wt. %)		Tensile strength (MPa)	Young's modulus (MPa)	Yield stress (MPa)	Stress at break (MPa)	Elongation at break (%)	Energy at break (J)	MFI (g/10 min)
	EVMT-1	PP							
C0	0	100	32.3 ± 1.3	911 ± 44	20.8 ± 0.9	30.6 ± 1.2	551 ± 22	8.32 ± 0.31	0.98 ± 0.04
C1	0.5	99.5	46.4 ± 1.6	1062 ± 48	26.3 ± 0.8	44.1 ± 2.0	529 ± 21	10.72 ± 0.50	1.19 ± 0.04
C2	1.0	99.0	49.9 ± 1.9	1162 ± 51	26.2 ± 0.9	47.4 ± 1.8	555 ± 23	12.0 ± 0.54	1.28 ± 0.05
C3	3.0	97.0	44.1 ± 1.8	1021 ± 54	21.2 ± 0.7	43.1 ± 1.5	511 ± 18	9.96 ± 0.46	1.34 ± 0.04
C4	5.0	95.0	44.0 ± 1.8	900 ± 43	21.1 ± 0.7	43.8 ± 1.7	505 ± 17	10.68 ± 0.50	1.57 ± 0.05

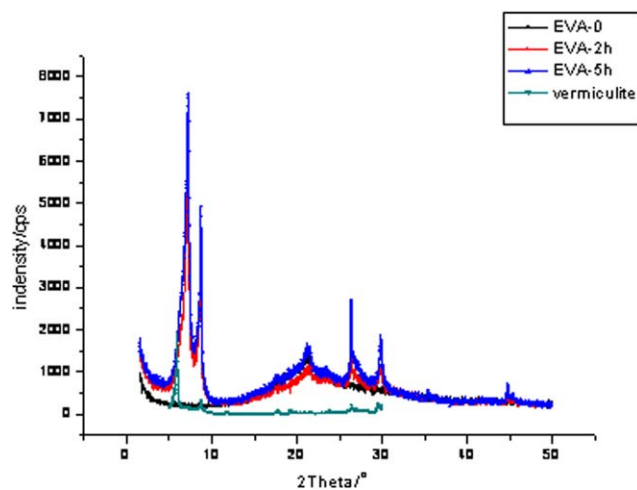


Figure 1. XRD patterns of EVMT, EVMT/EVA (ball milled in EVA latex for 2 and 5 h, respectively) and raw EVA. [Color figure can be viewed in the online issue, which is available at wileyonlinelibrary.com.]

Melting Flow Index Analysis. In accordance with the ISO 1133 standard, a 4–5 g PP sample was added to an MI-4 melting flow index (MFI) tester (Goettfert China) and preheated to 230°C. Next, a 2.16 kg weight was introduced onto the piston, and a sample of the melt was taken after a desired period of time to be weighed accurately. The MFI was expressed as grams of polymer/10 min.

OTR and WVTR Analysis. The rates of transmission of oxygen through CPP films were obtained using an Illinois 8001 oxygen permeation analyzer (Illinois Instruments, USA) at 25°C and 1 atm. The WVTR for CPP films were obtained using a Model OXTRAN 3/33 (Mocon, USA) during storage 38°C/100% RH.

Peel Strength of Flexible CPP Films. Two slices of 15 mm-wide CPP film samples were corona treated and laminated with two-component polyurethane adhesive, followed by a peel strength test, as per the ISO 11339:2003 standard.¹³ After the T-peel test was done on a 5565A Instron universal testing machine, the peel strength was determined by measuring the peeling force of a T-shaped bonded assembly of two laminated CPP films.

DMA Analysis. The DMA of the nano-modified PE film was performed using a dynamic mechanical analyzer (Model Q800, TA Instruments, USA) at a fixed frequency of 1 Hz and an amplitude of 20 μ m. The temperature studied ranged from –30 to 80°C, with a heating rate of 3°C/min.

Statistical Analysis. The mechanical properties and peel strength of each CPP film were measured for 10 times, followed by averaging and variance analysis, with confidence level of less than 0.05.

RESULTS AND DISCUSSION

Characterization of EVMT and EVMT/EVA

The XRD spectra of EVMT and organo-modified EVMT/EVA are presented in Figure 1.

The raw EVMT exhibits characteristic weak diffraction peaks (001) at 6.00°, which correspond to the basal spacing of 1.493 nm (XRD pattern in Figure 1). The $d(001)$ value of 1.493 nm in EVMT is

slightly higher than the d -spacing value of 1.435 nm reported for VMT,^{14,15} which relates to VMT expansion upon instantaneous heating to 1100°C. That is, crystal water and free water in the O layer and interlayer of VMT were rapidly vaporized at elevated temperature, and the water vapor expansion enlarged the spacing between the O layer and the interlayer of VMT, resulting in a higher $d(001)$ value (basal spacing) than those reported in the literature. After losing water, VMT sheets showed twist deformation, increased interplanar spacing, and macroscopic expansion and cleavage of VMT. Therefore, EVMT was characterized by reduced regular stacking along the c -axis, and the relative intensity of the (001) reflection decreased in comparison with raw VMT before expansion. This effect is related to increased tortuous sheet defects in EVMT and reduced grain size,¹⁶ so that the peak diffraction intensity of 001 in that plane is very low, resembling what has been reported in the literature.^{17,18} Even the d -spacing of 1.220 nm for hydrobiotite or hydrophlogopite (mixed-layer mica/VMT 1 : 1 layer) corresponding to reflection did not occur in the raw EVMT sample, owing to twist deformation induced by VMT plane dehydration. In comparison with findings from the literature,¹⁵ raw EVMT used in this experiment was instantaneously heated and held in the 1100°C furnace for less than 1 min; thus, most of the lost moisture is free water, and no dehydration occurred in the tetrahedral structure of hydrated Mg^{2+} in the O layer.

After EVMT had been ball milled in EVA latex for a period, the generated EVMT/EVA had greatly higher diffraction peak intensity than did EVMT before intercalation. These findings concur with the study by Holešova et al.¹⁹ Furthermore, the longer the ball-milling time, the greater the EVMT/EVA diffraction peak strength; that is, although diffraction peak positions of EVMT/EVA-5h and EVMT/EVA-2h did not change, EVMT/EVA-5h had greater diffraction peak intensity.

For VMT intercalated by EVA latex, as EVA resin was intercalated between the interlayer galleries, the $d(001) = 1.493$ nm basal spacing went beyond the measurement range. At the same time, no diffraction peaks between $2\theta = 1.5^\circ$ and 5° were seen in XRD spectra after intercalation. There were no diffraction peak at $2\theta = 7.019$ for EVMT samples, the corresponding phlogopite impurity in EVMT dehydrated to result in crystal deformation, since EVMT was treated at 1100°C; hence, the diffraction peak for phlogopite in EVMT disappeared. After EVMT was ball milled in EVA latex, the phlogopite sheet rehydrated to restore the original regular structure, so very strong diffraction peak of phlogopite appeared again in EVMT/EVA spectrum.

Table II also shows that the EVMT studied in this article (from the Qeganbulak VMT deposit) contains an impurity: hydrophlogopite, a kind of mica with a characteristic peak of $d(001) = 1.019$ nm.²⁰ The characteristic peaks of hydrophlogopite, at 1.019 and 0.337 nm, appeared at 1.016 and 0.337 nm in EVMT/EVA spectra, so almost no change occurred in both EVMT and EVMT/EVA samples. This finding indicates that micas have no interlayers and cannot be intercalated by EVA or water molecules, and their basal spacing does not change.

For EVA, PE segments in its main chain are relatively regular and can form a microcrystal structure, with weak diffraction

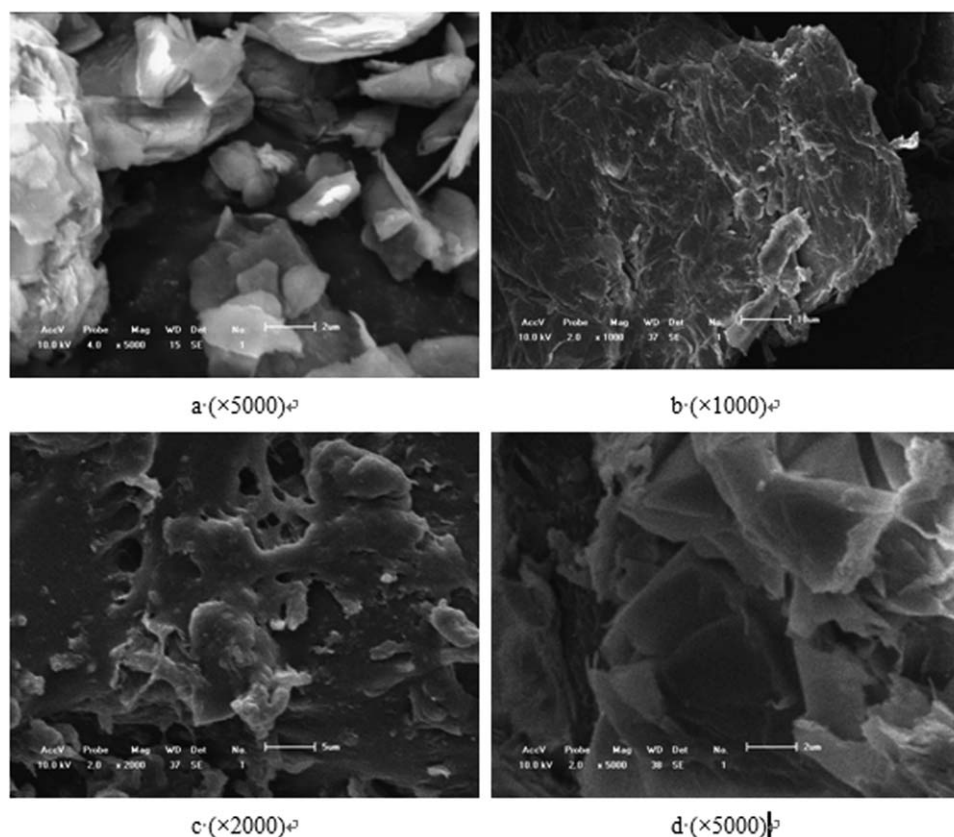


Figure 2. SEM images of (a) EVMT and (b–d) EVMT/EVA-2h.

peaks at 2θ angles of 21.3° and 23.7° (0.416 and 0.379 nm) in XRD, respectively, corresponding to (110) and (200) planes of PE microcrystal, respectively.^{21,22} The microcrystalline structures of these PE segments were retained in the EVMT/EVA composite.

Because VMT was instantaneously heated and expanded into EVMT [Figure 2(a)], the sheets were soon dehydrated and cleaved while maintaining a certain degree of order, without the necessity of being exfoliated into single sheets. For the sample EVMT/EVA-2h [subjected to 2 h ball milling in EVA latex and drying, Figure 2(b and c)], it was observed under 1000–2000 \times magnification that VMT had been bound and encapsulated by EVA resin. Under 5000 \times magnification [Figure 2(d)], it could be observed that the VMT's layered structure had become poorly ordered and cleaved, and that VMT had been intercalated by EVA and even exfoliated.

The OVMT derived from intercalating VMT with cetyltrimethylammonium bromide shared the same surface topography as our EVMT/EVA samples.¹⁸

Characterization of CPP Films

The EVMT-2h modifying agent prepared by 2 h ball milling was added to the PP matrix resin with VMT loadings at 0.2, 0.5, 1, and 2%, resulting in four modified CPP films. Next, their mechanical properties, crystallization properties, barrier properties, and peel strengths were tested and analyzed, and the influences of EVMT/EVA modifying agent content on CPP film properties were discussed.

Mechanical Properties. Table III shows that, compared with raw PP (C0), when EVMT-2h loading ranged between 0.5 and 1.0%, CPP film's strength and toughness increased

Table III. Positions of Diffraction Peaks of Neat EVMT, Neat EVA, and EVMT/EVA Nanocomposites

	VMT (001)	Phlogopite (002)	mica	VMT (002)	Phlogopite (003)	VMT (003)	EVA (110)	EVA (200)	VMT (004)	mica	VMT (005)
EVMT	2θ 6.00		8.77	11.81		17.81 19.22			23.63	26.50	29.99
	d 1.493		1.019	0.784		0.499 0.461			0.374	0.337	0.303
EVMT/EVA 2h, 5h	2θ	7.019	8.75		17.67		21.3	23.6		26.50	
	d	1.220	1.016		0.522		0.416	0.379		0.337	
EVA	2θ						21.3	23.6			
	d						0.416	0.379			

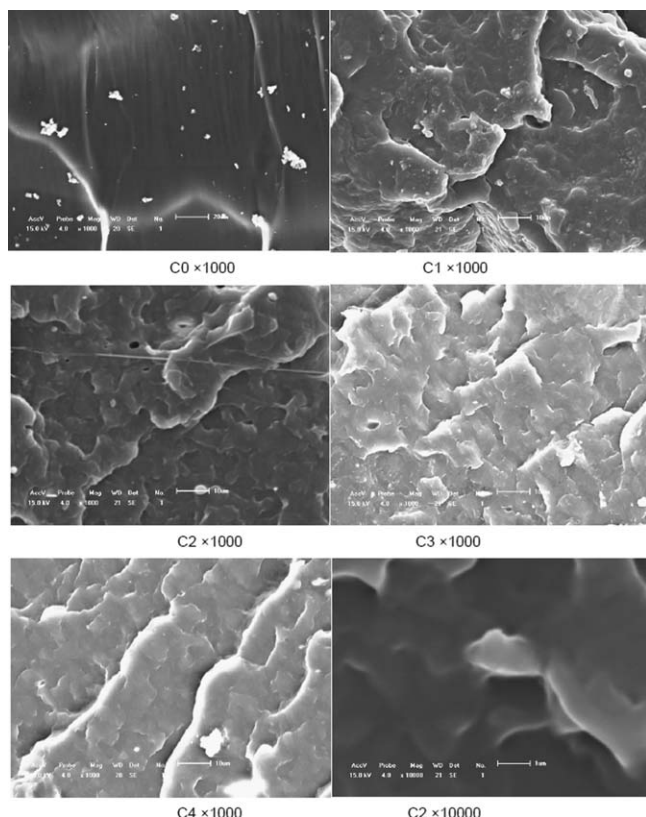


Figure 3. SEM micrographs of the fracture surfaces of neat CPP (C0) and four CPPs modified with EVMT-2h (C1–C4).

simultaneously along with increasing VMT content. This phenomenon manifested as a 44–54% rise in tensile strength, a 26% rise in yield stress, a 37–43% rise in stress at break, and a 29–34% rise in energy at break (i.e., toughness). These findings show that the effect of EVMT/EVA modifying is far better than that of conventional VMT/MAH modifying process,²³ in which, at VMT loading of 2–5%, tensile strength and Young's modulus of the VMT/MAH-modified PP resin increased by about 40–50%, but elongation at break and energy at break decreased to about 1/50 and 1/20 of the original ones, respectively. In our study, in case of EVMT-2h modifying agent, the effect at 3–5% loading was inferior to that at 0.5–1% loading, though the tensile strength and energy at break of the modified CPP still increased by 36% and 20%, respectively, when EVMT-2h loading was 3–5%. Meanwhile it is also found that, when EVMT-2h loading was 3–5%, mechanical properties such as tensile strength and yield stress were not so well improved as in the cases of samples C1 and C2, due to poorer dispersion of EVMT sheets in CPP, nonetheless, they were distinctly better than those of sample C0.

The improved mechanical properties of EVMT-modified CPP originate from good dispersion effect of EVMT in the PP matrix resin. As can be seen from Figure 3, C0 (neat CPP, 1000 \times) has flat fracture surfaces with few fracture dimples. In contrast, the EVMT-2h modified CPP has improved toughness, more fracture dimples and shear zones, and closer bonding between VMT and PP matrix. As observed in a 10,000 \times micrograph of C2, there

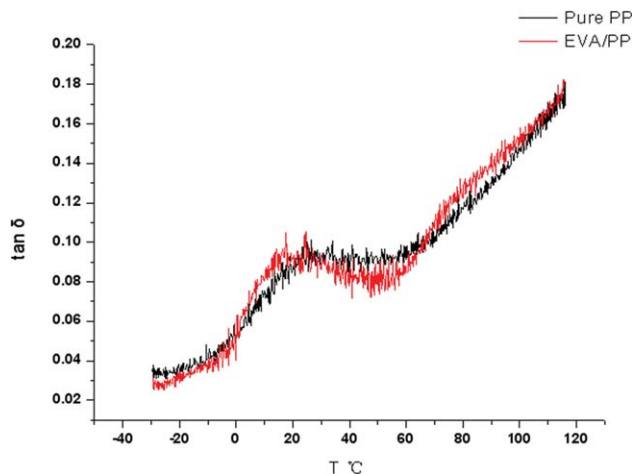


Figure 4. Curves of $\tan \delta$ versus temperature (T) for neat (pure) PP and an EVA/PP blend composite. [Color figure can be viewed in the online issue, which is available at wileyonlinelibrary.com.]

is no phase interface between VMT and PP matrix resin on the edges of VMT, implying that PP resin and VMT are closely bound and strong intermolecular force occurs in between; thus, VMT has the effect of reinforcing PP, which can explain why the PP's mechanical properties have been improved.

In general, VMT (or MMT) and PP differ dramatically in polarity, and their compatibility is poor. Therefore, PP-grafted MAH is generally used as a compatibilizer to improve the dispersion of VMT in PP.^{24–26} In this study, we adopted water-based EVA resin (latex) as the compatibilizer. The content of VA segment in this brand of EVA resin is more than 50%, and the polar VA segment has good affinity to polar VMT. Furthermore, the EVA resin itself has relatively good compatibility with the amorphous zone of PP. Figure 4 shows that the T_g of neat PP is 27.7 $^{\circ}\text{C}$, whereas the T_g of the PP/EVA blend composite containing 8% EVA decreases to 22.3 $^{\circ}\text{C}$. This finding indicates that there is definite intermolecular force between amorphous EVA and the amorphous zone of PP, so EVA and PP have relatively good compatibility. The issue of EVA-PP compatibility has been studied by other researchers, too. For instance, Ramírez-Vargas²⁷ studied two blend systems, polypropylene–(ethylene–propylene) heterophasic copolymer (PP–EP)/EVA, and PP/EVA; for the PP–EP/EVA blends, interfacial interactions in amorphous zones, which were associated with shifts in T_g , indicate that PP–EP is relatively well compatible with EVA, for both macromolecules contain ethylene segment. Despite that Dikobe and Luyt²⁸ regarded EVA and PP as completely incompatible, we came to a conclusion that transition of T_g of PP in PP/EVA system indicates that EVA and PP are compatible in amorphous zones; such contradiction occurs possibly because Dikobe and Luyt selected different PP and EVA raw materials from those we used.

Because polar EVA molecules have excellent compatibility with VMT, they intercalate the VMT quite easily. However, during melt blending of EVMT/EVA and PP, the EVMT/EVA was subjected to shear, and VMT sheets started to be exfoliated and encapsulated by EVA and dispersed within the PP matrix. The

Table IV. Crystallization Properties of Modified CPPs

Specimen	Vermiculite content (%)	Crystallization enthalpy (J/g)	Peak value (°C)	Onset point (°C)	End-set point (°C)	Crystallization width (°C)	Degree of crystallinity (%)
C0	0	-88.74	116.70	119.93	112.97	6.96	53.78
C1	0.5	-88.57	115.84	118.78	111.96	6.82	53.68
C2	1	-88.38	116.16	119.12	112.08	7.04	53.56
C3	3	-87.52	115.42	118.27	111.33	6.94	53.04
C4	5	-86.91	115.54	118.38	111.65	6.73	52.67

micrographs of C2 (Figure 3) show that no phase interface appears around the edges of the VMT sheets. Indeed, the dispersion state of VMT seen here is quite similar to SEM micrographs of VMT sheets in VMT-modified PP samples prepared by solid state shear compounding using pan-mill equipment,³ or using MAH-grafted copolymer as the compatibilizer.²³ These findings indicate that, using EVA as the intercalating agent and compatibilizer, one can prepare modified PP material that is more compliant with food safety standard. Moreover, the mechanical properties of the modified PP in this study are better than those of similar VMT-modified PP.

VMT has positive impact on PP's mechanical properties, which can also be validated by DSC analysis of CPP. As can be seen from the characteristics of neat PP and modified CPPs (C1–C4) in Table IV, adding VMT has not hampered PP crystallization. In addition, the modification has no significant influence on parameters such as crystallinity, onset crystallization temperature, end-set crystallization temperature, and crystallization half-peak width. In most cases, if the added modifying agent does not induce heterogeneous nucleation in the matrix, then PP crystallization must definitely be hampered, leading to a reduction in onset crystallization temperature and crystallinity of PP, and narrowing in crystallization half-peak width. In this study, VMT displayed distinct heterogeneous nucleation, both reinforcing and toughening PP.

Influence of VMT Modification on MFI. Introducing inorganic particles into a macromolecular polymer generally leads to a rise in system viscosity. For spherical particles, the relationship between viscosity and inorganic particle loading conform to the Einstein equation²⁹:

$$\eta/\eta_0 = 1 + 2.5\phi \quad (1)$$

where η_0 and η are system viscosities before and after adding spherical nanoparticles, and ϕ is the volume fraction of nanoparticles.

For a layered silicate nanocomposite dispersion system such as VMT, van Olphen³⁰ proposed the following formula for large thin disks with small aspect ratios:

$$\eta_{sp} = \frac{32\phi}{15\pi p} \quad (2)$$

where p is the aspect ratio.

In general, adding rigid platelet VMT particles would undoubtedly increase PP's Young's modulus while increasing the viscos-

ity of the PP composites substantially. However, it can be seen from MFI data in Table II that, at 0.5–5% VMT loading, the melt viscosity of modified PP decreased instead. Also, the magnitude of this decrease became greater with increasing VMT loading, manifesting as a reduction in MFI value. Although this finding seems to contradict the current theory of rigid particle filling and tackifying, considering the amorphous EVA structure that exists among the EVMT/EVA/PP composites at a mixing ratio of 1 : 3 with VMT, it is very easily interpreted. DMA has shown that EVA has excellent compatibility with the BOPP special materials used in this experiment, a low melting point and flexible EVA molecule chain serves as a plasticizer in the PP matrix to lower the activation energy for viscous flow of the PP molecule chain. Also, the reduction in viscosity of the EVMT/PP composites is greater than EVMT's tackifying effect on PP. Thus, as a whole, the EVA/EVMT/PP composites show a trend of falling viscosity with increasing EVMT loading. This quality is favorable for processing and forming EVA/EVMT-modified CPP films.

Barrier Properties of Modified CPPs. Layered silicate shows enhanced gas barrier properties in many packaging materials, such as polylactide,³¹ polymethyl methacrylate,³² and PA.³³ The improved barrier properties of polymer clay nanocomposites seem to result from an increased tortuosity of the permeant diffusion path, which forces them to travel a longer path to diffuse through the film. This theory was developed by Nielsen,³⁴ who postulated that the ratio of the gas transmission rate of a nanocomposite to that of raw polymer film follows the following formula:

$$\frac{K_{\text{composite}}}{K_{\text{matrix}}} = \frac{1-\phi}{1+(\alpha/2)\phi}, \quad (3)$$

where ϕ is the volume fraction of filler and α is the aspect ratio (length divided by width) of the individual filler particle. The α value of platelet nano-VMT can range from 100 to 500.^{35,36} Later, many scholars derived other types of mathematical expressions as to how platelet particles affect barrier property of PP, for instance, Wakeham and Mason proposed the Cussler model,³⁷ which was then revised by Falla et al.³⁸ who developed the Falla model. Nonetheless, we still used the simplest Nielsen model to fit the change trend of modified CPP film's barrier property.

The bigger the aspect ratio of nanoparticle packaging material, the higher contribution it makes to the barrier property. Adding 0.50–5.0% of EVMT-2h to PP gives rise to CPP film; at EVMT

Table V. Barrier Property and Peel Strength of Modified CPPs

Specimen	Vermiculite content (%)	Thickness (μm)	OTR $\text{mL}/(\text{m}^2\cdot\text{day}\cdot 0.1 \text{ MPa})$			WVTR $\text{mg}/(\text{m}^2\cdot\text{day}\cdot 0.1 \text{ MPa})$
			Theoretical value	Experimental value	Relative error %	
C0	0	40	1219.4	1219 ± 61	0	7.31 ± 0.32
C1	0.5	41	1103.0	1144 ± 48	3.7	7.32 ± 0.29
C2	1.0	41	1006.0	1062 ± 52	5.5	7.56 ± 0.35
C3	3.0	40	739.2	1419 ± 60	/	17.89 ± 0.31
C4	5.0	40	579.2	1461 ± 59	/	20.52 ± 0.55

loading of 0.5–1.0%, the OTRs of modified CPP films decreased by 6.2–12.9% (Table V), which is in excellent conformity with Nielsen model. The fitted aspect ratio of VMT in the EVMT/PP composite amounts to 40, and the error between experimental value and theoretically calculated value according to the Nielsen model ranges from 3.7 to 5.5%. Note, however, that at 3.0–5.0% loading, experimental values deviate from the Nielsen model. By contrast, the OTR of modified CPP film with an EVMT loading of 3.0–5.0% actually increases, because at high EVMT loading, its dispersion state in the PP matrix is not good, and macroscopic defects form on the film surface, causing the gas permeability to rise instead.

When EVMT loading is 0.5–1%, the WVTR of EVMT-modified CPP does not significantly affect. However, this does not indicate that EVMT has no barrier effect on water vapor, because in fact, the gas transmission rate K of the film is related to the coefficient of diffusion D and gas solubility S of the film matrix. This satisfies the following equation³⁹:

$$K = S \times D, \quad (4)$$

where S is the solubility, and D is the diffusion coefficient.

The addition of EVMT can prolong the gas transmission path or reduce gas diffusivity D in the matrix. However, hydrophilic VMT in a PP matrix will increase the solubility of water vapor in the film. When EVMT loading is 0.5–1%, EVMT enables a trade-off between a reduction in the coefficient of diffusion (D) and a rise in solubility (S) of water vapor; thus, its impact on WVTR is not significantly (Table V). But when EVMT loading is 3–5%, WVTR rises by 1–2 times, because macroscopic film defects increase, and the VMT dispersion state worsens, as a resulting in high rise in solubility (S) of water vapor in modified CPP film while the coefficient of diffusion D remains

high. Therefore, when EVMT loading was more than 3%, the WVTR of modified CPP film exhibited a linear increase.

Peel Strength After Lamination with Modified CPP. Peel strength after lamination is a critical factor of packaging quality. It is generally required that the peel strength of food packaging film should be greater than 1.5 N/15 mm. CPP often serves as the heat-sealing layer of flexible food packaging, and is laminated with a printing layer or other high-barrier layer using Polyurethane (PU) or acrylic adhesive. Because the polarity of the adhesive is generally much higher than that of PP film, the van der Waals force (bond) between CPP film and adhesive is, in theory, relatively weak. Thus, the CPP film surface needs to be corona treated before lamination to enhance CPP polarity and thus increase the van der Waals force between CPP and the polar adhesive so as to raise peel strength. No doubt, adding polar VMT will increase the polarity of modified CPP and the van der Waals force between modified CPP and polar adhesive, thereby improving the peel strength of modified CPP films.

After two CPP films were laminated using PU adhesive, the peel strength of C1 sample film rose by 27% relative to C0, and that of C2 gained 18% relative to C0 (Table VI). In contrast, when VMT loading exceeded 3%, the composite strengths of CPP samples C3 and C4 decreased instead. Because plastic surface is rugged when VMT content is equal or greater than 3%, it is difficult for the adhesive to fully adhere to the film (Figure 5), causing its composite strength to fall dramatically.



Figure 5. Surface topography of C4 film after peeling. The bright portions are PU adhesive, while the dark portions represent the CPP film substrate not coated with PU adhesive. [Color figure can be viewed in the online issue, which is available at wileyonlinelibrary.com.]

Table VI. Peel Strength of Modified CPPs

Specimen	Vermiculite content (%)	Thickness (μm)	Peel force (N/15 mm)
C1	0.5	41	6.70 ± 0.28
C2	1.0	41	6.25 ± 0.26
C3	3.0	40	2.75 ± 0.12
C4	5.0	40	1.25 ± 0.10

CONCLUSIONS

The process of preparing OVMT by ball-milling EVMT in water-based EVA latex enables VMT exfoliation. EVA acts as the VMT-PP compatibilizer, and shear force during melt blending with PP enables VMT sheets to be exfoliated and well dispersed throughout the PP matrix. As a physical crosslinking point, EVMT enhances the mechanical properties of modified CPP compared with raw PP (C0). When EVMT loading was between 0.5% and 1.0%, the strength and toughness of CPP film increased simultaneously with increasing VMT content. This effect manifests as tensile strength increasing by 44–54%, yield stress increasing by 26%, stress at break increasing by 37–43%, and energy at break (toughness) increasing by 29–34%. Even when EVMT content was 3–5% and the VMT dispersion effect was poor, tensile strength and energy at break still increased by 36 and 20%, respectively. EVMT enhances CPP film's barrier properties: the OTR of modified CPP film decreased by 6.2–12.9% and the WVTR was not significantly affected at EVMT loading of 0.50–1.0%. However, when EVMT content is 3–5%, barrier property of the modified CPP film decreased instead, with OTR and WVTR rising by 15% and more than 100%, respectively. In addition, when EVMT loading was 0.5–1%, the peel strength of CPP film increased by 20%; but at EVMT loading of 3–5%, peel strength of CPP film decreased greatly instead. At EVMT loading of 0.5–1%, MFI of modified CPP increased with elevated loading, such attribute help accelerate processing speed, resulting in improved processing property of EVMT/EVA/PP composite. However, when EVMT loading is 3–5%, MFI of modified CPP decreased with increasing loading instead.

ACKNOWLEDGMENTS

This work was financially supported by Beijing Municipal Science and Technology Commission Project (Grant No. Z101103053210058), Institute-Level Disciplinary Construction and Postgraduate Education Project (Grant No. 21090112001), and Beijing Municipal Education Commission Project on Three-dimensional Printing Technology.

REFERENCES

- Schneider, T. Days of Packaging Knowledge. Available at: <http://www.festacropak.hr/en/congres/>. Accessed date 15 July 2012.
- Valášková, M.; Martynková, G. S. Vermiculite: Structural Properties and Examples of the Use. Available at: <http://dx.doi.org/10.5772/51237>. Accessed date 12 September 2012.
- Shao, W.; Wang, Q.; Chen, Y.; Y. Gu. *Mater. Manuf. Processes* **2006**, *21*, 173.
- Pereira de Abreu, D. A.; Paseiro Losada, P.; Angulo, I.; Cruz, J. M. *Eur. Polym. J.* **2007**, *43*, 2229.
- Han, W.; Li, Z.; Wang, Z.-Q.; Yang, H.-Q. *Polym. Plast. Technol. Eng.* **2009**, *48*, 374.
- Zhang, Y.; Han, W.; Wu, C.-F. *J. Macromol. Sci. B* **2009**, *48*, 967.
- Martynková, G. S.; Valášková, M.; Capková, P.; Matejka, V. *J. Colloid Interface Sci.* **2007**, *313*, 281.
- Mališ, J.; Křístková, M. *Acta Geodyn. Geomater.* **2005**, *2*, 105.
- Goodarzi, V.; Jafari, S. H.; Khonakdar, H. A.; Monemian, S. A.; Mortazavi, M. *Polym. Degrad. Stab.* **2010**, *95*, 859.
- Goodarzi, V.; Jafari, S. H.; Khonakdar, H. A.; Ghalei, B.; Mortazavi, M. *J. Membr. Sci.* **2013**, *445*, 76.
- Chen, L.; Wong, S.-C.; Pisharath, S. *J. Appl. Polym. Sci.* **2003**, *88*, 3298.
- Mandelkern, L.; Alamo, R. G. In *Physical Properties of Polymers Handbook*; Mark, J. E., Ed.; American Institute of Physics: New York, **1996**.
- Takahashi, J.; Nakamura, Y.; Hotta, A. *Polym. Prepr.* **2011**, *52*, 372.
- Suquet, H.; Chevalier, S.; Marcilly, C.; Barthomeuf, D. *Clay Miner.* **1991**, *26*, 49.
- Michot, L. J.; Tracas, D.; Lartiges, B. S.; Lhote, F. *Clay Miner.* **1994**, *29*, 133.
- Valášková, M.; Simha Martynková, G.; Matějka, V.; Barabaszová, K.; Plevová, E.; Měřínská, D. *Appl. Clay Sci.* **2009**, *43*, 108.
- El Mouzdahir, Y.; Elmchaouri, A.; Mahboub, R.; Gil, A.; Korili, S. A. *Powder Technol.* **2009**, *189*, 2.
- Wang, L.; Chen, Z.; Wang, X.; Yan, S.; Wang, J.; Fan, Y. *Appl. Clay Sci.* **2011**, *51*, 151.
- Holešova, S.; Valášková, M.; Plevova, E.; Pazdziora, E.; Matejova, K. *J. Colloid Interface Sci.* **2010**, *342*, 593.
- Huo, X.; Wu, L.; Liao, L.; Xia, Z.; Wang, L. *Powder Technol.* **2012**, *224*, 241.
- van Laarhoven, H.; Veurink, J.; Krufft, M.-A.; Vromans, H. *Pharm. Res.* **2004**, *21*, 1811.
- Goderis, B.; Reynaers, H.; Scherrenberg, R.; Mathot, V.; Koch, M. *Macromolecules* **2001**, *34*, 1779.
- Tjong, S. C.; Meng, Y. Z.; Hay, A. S. *Chem. Mater.* **2002**, *14*, 44.
- Xu, W.; Liang, G.; Zhai, H.; Tang, S.; Hang, G.; Pan, W.-P. *Eur. Polym. J.* **2003**, *39*, 1467.
- Chen, C.; Baird, D. G. *Polymer* **2012**, *53*, 4178.
- Sharma, S. K.; Nayak, S. K. *Polym. Degrad. Stab.* **2009**, *94*, 132.
- Ramírez-Vargas, E.; Medellín-Rodríguez, F. J.; Navarro-Rodríguez, D.; Avila-Orta, C. A.; Solís-Rosales, S. G.; Lin, J. S. *Polym. Eng. Sci.* **2004**, *42*, 1350.
- Dikobe, D. G.; Luyt, A. S. *Express Polym. Lett.* **2009**, *3*, 90.
- Einstein, A. *Ann. Phys. (Leipz.)*. **1906**, *19*, 371.
- van Olphen, H. *Clay Colloid Chemistry*; Wiley: New York, **1977**.
- Singh, S.; Gupta, R.; Ghosh, A.; Bhattacharya, S.; Maiti, S. *J. Polym. Eng.* **2010**, *30*, 361.
- Yeh, J.-M.; Liou, S.-J.; Lai, M.-C.; Chang, Y.-W.; Huang, C.-Y.; Chen, C.-P.; Jaw, J.-H.; Tsai, T.-Y.; Yu, Y.-H. *J. Appl. Polym. Sci.* **2004**, *94*, 1936.
- Pereira, D.; Losada, P. P.; Angulo, I.; Greaves, W.; Cruz, J. M. *Polym. Compos.* **2009**, *30*, 436.

34. Nielsen, L. E. *J. Macromol. Sci. Pure Appl. Chem.* **1967**, *1*, 929.
35. Kaylo, A. J.; Karabin, R. F.; Lan, T.; Sandala, M. G. Curable coating compositions containing high aspect ratio clays. WO2000049082A1. **2000**, USA.
36. Arora, A.; Padua, G. W. *J. Food Sci.* **2010**, *75*, 43.
37. Wakeham, W. A.; Mason, E. A. Diffusion through Multiperforate Laminae, *Ind. & Eng. Chem. Fund.* **1979**, *18*, 301.
38. Falla, W. R.; Mulski, M.; Cussler, E. L. *J. Membr. Sci.* **1996**, *119*, 129.
39. Kanehashi, S.; Kusakabe, A.; Sato, S.; Nagai, K. *J. Membr. Sci.* **2010**, *365*, 40.